

1 **Will daytime community calcification reflect reef accretion on**
2 **future, degraded coral reefs?**

3 Coulson A. Lantz^{1,2}, William Leggat², Jessica L. Bergman¹, Alexander Fordyce², Charlotte Page¹,
4 Thomas Mesaglio¹, Tracy D. Ainsworth¹

5 ¹University of New South Wales, School of Biological, Earth and Environmental Sciences, Kensington, 2033 NSW
6 Australia

7 ²University of Newcastle, School of Environmental and Life Sciences, Callaghan 2309 NSW Australia

8 Email Corresponding Author: C.lantz@unsw.edu.au

9 **Abstract**

10 Coral bleaching events continue to drive the degradation of coral reefs worldwide, causing a shift in
11 the benthic community from coral to algae dominated ecosystems. Critically, this shift may decrease
12 the capacity of degraded coral reef communities to maintain net positive accretion during warming-
13 driven stress events (e.g., reef-wide coral bleaching). Here we measured rates of net ecosystem
14 calcification (NEC) and net ecosystem production (NEP) on a degraded coral reef lagoon community
15 (coral cover < 10 % and algae cover > 20 %) during a reef-wide bleaching event in February of 2020
16 at Heron Island on the Great Barrier Reef. We found that during this bleaching event, rates of NEP
17 and NEC across replicate transects remained positive and did not change in response to bleaching.
18 Repeated benthic surveys over a period of 20 d indicated an increase in the percent area of bleached
19 coral tissue, corroborated by relatively low Symbiodiniaceae densities ($\sim 0.6 \times 10^6 \text{ cm}^{-2}$) and dark-
20 adapted photosynthetic yields in photosystem II of corals (~ 0.5) sampled along each transect over this
21 period. Given that a clear decline in coral health was not reflected in the overall NEC estimates, it is
22 possible that elevated temperatures in the water column that compromise coral health enhanced the
23 thermodynamic favourability for calcification in other ahermatypic benthic calcifiers. These data
24 suggest that positive NEC on degraded reefs may not equate to the net positive accretion of reef
25 structure in a future, warmer ocean. Critically, our study highlights that if coral cover continues to
26 decline as predicted, NEC may no longer be an appropriate proxy for reef growth as the proportion of
27 the NEC signal owed to ahermatypic calcification increases and coral dominance on the reef decreases.

28 **1. Introduction**

29 Corals have long been the focus of climate change research in tropical oceans, as they are a keystone
30 species responsible for the biogenic construction of reef habitat (Grigg and Dollar, 1990). Adverse
31 effects to their ability to secrete calcium carbonate structure have negative implications for coral reef
32 ecosystems, given corals are the major organism responsible for collectively maintaining the
33 accumulation of permanent reef structure at a rate that overcomes the biological and physical
34 mechanisms which act to break reefs down (carbonate dissolution, bioerosion, storm activity; Eyre et
35 al., 2018). In contrast to coral-derived calcium carbonate, other benthic marine calcifiers, such as non-
36 sessile Gastropods, Echinoderms, or Halimeda algae (Ries et al., 2009; Harney and Fletcher, 2007),
37 secrete calcium carbonate which is relatively temporary and does not contribute to the long-term reef
38 structure. Traditionally, corals are classed as the dominant calcifier on tropical coral reefs, occupying
39 between 10 – 50 % of benthic area in healthy coral reef lagoons (Bruno and Selig, 2007; Brown et al.,
40 2018). As such, estimates of net ecosystem calcification (NEC) are considered synonymous with the
41 growth and function of the entire coral reef community and can be used to represent the collective
42 response in coral reef community health to anthropogenic stressors such as ocean warming and
43 subsequent reef-wide bleaching events (Courtney et al., 2018).

44 Presently, records of coral reef NEC during a reef-wide bleaching event (driven by sea surface
45 temperatures + 1 °C above monthly maximum means; Heron et al., 2016; Sully et al., 2019) are rare
46 (McMahon et al., 2019). The effects of bleaching events, and their associated thermal seawater
47 temperature anomalies, on coral reef NEC have been predominately studied *ex-situ* using recreated
48 communities in aquaria (Dove et al., 2013) or scaling up the response from organism-level studies,
49 both *ex-* (Castillo et al., 2014) and *in-situ* (Cantin et al., 2010). In studies conducted *ex-situ* in aquaria,
50 a warming treatment strong enough to cause bleaching (between 1 – 4 °C above the summer mean)
51 reduced coral calcification rates by 30 to 90 % (Cantin et al., 2010; D’Olivo and McCulloch, 2017).
52 *In-situ* observations following bleaching events have shown a 20 – 90 % reduction in individual coral

53 calcification rates (Castillo et al., 2014) and a significant reduction in the coral endosymbiont
54 photosynthetic yields (evidence of damage to their photosystems; Warner et al., 1999). At the whole
55 community level, the few *in-situ* studies which have observed community metabolism during a
56 bleaching event recorded a 40 % (DeCarlo et al., 2017; Dongsha Atoll, Taiwan) to 100 % (Courtney
57 et al., 2018; Kaneohe Bay, Hawai'i; Kayanne et al., 2015; Palau) decline in reef NEC. This effect that
58 has been observed to linger six to twelve months after these events, with NEC remaining depressed by
59 as much as 40 – 46 % (Lizard Island; McMahon et al., 2019) and an ultimate loss of 30 – 90 % of the
60 benthic coral cover (Brown and Suharsono, 1990; Baird et al., 2002). Experiments with simulated
61 communities in aquaria (e.g., Dove et al., 2013) validate these organism- and community-level *in-situ*
62 studies, where this same magnitude of warming lead to a reduction in the experimental community
63 coral cover by 30 %, a 70 % decline in NEC, and subsequent out-competition of corals by neighbouring
64 algae.

65 The overgrowth of algae has been mirrored in the natural reef lagoon environment several times
66 following bleaching events (Hughes et al., 1999; Diaz-Pulido et al., 2009). Despite a recovery to
67 normal pre-disturbance NEC within two years following a 2014 bleaching event at Lizard Island
68 (Pisapia et al., 2019), there was a permanent shift from coral to algae as the dominant benthic
69 community member, with a decline in coral cover from 8 % to 3 % along transects established at the
70 southeast end of the lagoon (McMahon et al., 2019). This response has been seen elsewhere on the
71 Great Barrier Reef, where reef-wide bleaching events lead to the overgrowth of unpalatable *Lobophora*
72 *vareigata* algae (Diaz-Pulido et al., 2009) to the extent that coral became a minority constituent (~ 2 –
73 5 %) in the lagoon's benthic community. This transition to an algal-dominated reef community
74 jeopardizes the efficacy of NEC as a proxy for reef growth given that hermatypic corals can no longer
75 be considered the dominant benthic organism (Courtney et al., 2018). Similar questions have been
76 raised after other anthropogenically-driven stress events (e.g., eutrophication and sedimentation;
77 Edinger et al., 2000) where coral growth rates on undisturbed reefs did not differ from those measured

78 on polluted, algal-dominated reefs where habitat structure was clearly degrading. If the community
79 predominantly becomes covered in algae and the habitat structure is visibly degrading, does NEC still
80 represent reef growth or does it now reflect a greater proportion of ahermatypic organism calcification
81 not contributing to permanent structure?

82 Shift from coral to algal dominated reefs without the concomitant decline in NEC have been observed
83 by Kayanne et al., (2005; 7.1 % coral cover), where no change in NEC on Shiraho Reef, Japan was
84 measured despite 51 % of the corals bleaching during a 1998 bleaching event and a decline to 5.8%
85 coral cover. This study suggested that continued calcification by living, unbleached corals, calcifying
86 algae, or other benthic calcifiers (e.g., foraminifera, gastropods, echinoderms) may have compensated
87 for any expected bleaching-driven decline in coral calcification. This discrepancy between Kayanne et
88 al., (2005; no change in NEC on a reef with < 10 % coral cover) and that of other NEC estimates during
89 a bleaching event (decline in NEC on a reef \geq 10 % coral cover; DeCarlo et al., 2014) may be due to
90 a critical threshold in the relationship between NEC and percent coral cover. This is of specific concern
91 when using NEC to monitor community function (i.e., the net accretion of reef structure) during coral
92 bleaching or other disturbance events on future, degraded reefs where algae will likely become the
93 dominant benthic member.

94 To address these emerging concerns, this study investigated community metabolism on a degraded
95 coral reef community (coral cover < 10 %, algae cover > 20 %) during a bleaching event at Heron
96 Island on the Great Barrier Reef in February of 2020. Flow-metabolism transects were established on
97 two areas within the Heron Island lagoon and estimates of community metabolism (NEP and NEC),
98 coral metaorganism function (photosynthetic yields, Symbiodiniaceae densities), benthic cover, and
99 bleaching extent (percent bleached coral tissue) were assessed during the period of peak thermal stress.

100 **2. Materials and Methods**

101 **2.1 Study Area**

102 This study was conducted from January 15th to February 10th of 2020. Two separate 200m x 100m
103 lagoon sites (Lagoon site 1 and 2; Fig.1) which each differed in total coral cover were established on
104 the southern side of the Heron Island lagoon (23° 26'670' S, 151° 54.901' E). Community metabolism,
105 physiochemical data, benthic community cover, and bleaching extent were then repeatedly measured
106 on each transect over a period of 20 days. HOBO temperature loggers (Onset, USA), which recorded
107 temperature (°C) at an interval of 15 minutes, were deployed at nine upstream and downstream
108 locations (1 - 9) across the study area (Fig. 1). Overlapping loggers located at the middle deployment
109 locations (2, 5, and 8) were used for both Lagoon site 1 and 2, resulting in six loggers per site.

110 To measure the accumulation of temperature stress above the local bleaching threshold (defined here
111 as the Maximum of the Monthly Means, MMM + 1 = 28.3 °C; Liu et al. 2014;) mean temperatures
112 across all nine loggers were used to calculate the number of Degree Heating Weeks (DHWs), which
113 represents the 12-week accumulation of temperatures above the MMM (Heron et al., 2016). Because
114 HOBO temperature loggers may record higher temperatures than surrounding seawater due to internal
115 heating of the transparent plastic casing (Bahr et al., 2016), HOBO loggers were deployed in the shade
116 on a cinderblock and downloaded temperature data were corrected for precision (48-h side-by-side
117 logging of all nine loggers in an aquarium) and accuracy (deployment next to Hanna HI98194
118 multimeter recording temperature). Light loggers (2π Odyssey PAR sensor) were deployed within the
119 middle of each study site (n = 1 site⁻¹). Loggers were attached to a star picket to ensure the sensor was
120 exactly 20 cm above the benthos and recorded light intensity at 15-minute intervals. Odyssey light
121 logger data were converted to μmol quanta of photosynthetic active radiation (PAR) m⁻² s⁻¹ using a
122 linear calibration over a 24-h period with a 2π quantum sensor LI-190R and a LiCor LI-1400 meter
123 (R² = 0.92).

124 **2.2 Benthic Community Surveys**

125 The benthic community along each 200 m transect was described using four survey approaches: 1)
126 Point-contact surveys, 2) Photo-quadrat surveys, 3) Mobile invertebrate counts, and 4) Invertebrate

127 and algal taxonomy descriptions. For the 1) Point-contact surveys and 2) Photo-quadrat surveys,
128 benthic cover was categorized as coral (hermatypic, live), coral (bleached), coral (soft), algae (fleshy,
129 non-calcifying), other calcifier (e.g., *Halimeda* spp.), rubble, and sediment. For the point-contact
130 method, the occupier of benthic space was recorded underneath each 1 m interval ($n = 200$ transect⁻¹)
131 at the beginning and end of the study and data are presented as relative % cover. These surveys were
132 repeated twice per transect at the beginning of the study (Jan 18-20 2020) to provide an initial
133 understanding of the community structure prior to flow-metabolism measurements. For the 2) photo-
134 quadrat method, a photo of a 1 m² PVC quadrat was taken at every 5 m interval ($n = 40$ transect⁻¹)
135 three times throughout the study: 1) at the beginning prior to any observed bleaching (Jan 24 2020), 2)
136 in the middle after the first observed bleaching event (Feb 6 2020), and 3) at the end of the study after
137 several more observed bleaching incidents (Feb 13 2020).. These images were analysed in ImageJ
138 using one side of the photo quadrat to set the scale (1 m) and the area tracing tool calculate the relative
139 % area of each category over time.

140 For mobile invertebrate surveys, a transect tape was laid along each 200 m transect length relatively
141 large, easily visible mobile invertebrates (e.g., sea cucumbers, sea hares, sea urchins) located 1 meter
142 to the left or right along the transect were counted. Surveys were conducted at dawn to ensure a balance
143 of visibility and invertebrate activity and repeated 3 times along each transect ($n = 9$ site⁻¹). Data are
144 presented as abundance counts per m² (individuals m⁻²). Individuals present at less than 0.1 m⁻² were
145 excluded from the final data reported but were included as part of the invertebrate taxonomy described
146 below. For general invertebrate taxonomy, while conducting the survey approaches detailed above,
147 each time a new invertebrate morphospecies was encountered, photographs were taken and uploaded
148 to iNaturalist, a biodiversity citizen science platform where identifications are contributed in real time
149 by both amateur naturalists and professional taxonomists as part of a consensus system
150 (www.inaturalist.org). Using a combination of taxonomic keys and crowdsourcing via iNaturalist,
151 algae, corals, and other sampled marine invertebrates were identified to as fine a taxonomic level as

possible. These data are presented as presence/absence across the entire 200 m x 400 m study area. Because sampling was conducted at low tide, most fish usually present in the lagoon were absent and excluded from benthic survey data.

2.3 Bleached Coral Physiology

Following the qualitative appearance of bleaching (white corals in photo quadrat surveys), efforts were made to provide physiological data that would corroborate bleaching observations. This was accomplished through Symbiodiniaceae density analyses for both *Acropora* spp. (*Acropora aspera*, *Acropora millepora*, *Acropora muricata*, *Acropora humilis*) and “Other” corals (*Pocillopora damicornis*, *Isopora palifera*, *Porites cylindrica*, *Montipora digitata*). For photophysiology, replicate coral fragments (n = ~15 - 35 time point⁻¹) of both *Acropora* spp. and “Other” corals were collected across all transects at Lagoon site 1 and 2 by hand on Feb 4 and Feb 9, 2020 (once bleaching was apparent) and used to measure photosynthetic efficiency of in hospite Symbiodiniaceae cells. Measurements of photosystem II dark-adapted yield were taken using a Pulse-Amplitude Modulated (PAM) fluorometer (MAXI Imaging PAM, Waltz, Effeltrich, Germany) using imaging PAM analysis (n = 3 technical replicates per fragment).

For quantification of Symbiodiniaceae densities, replicate coral fragments (n = ~15 - 35 time point⁻¹) of both *Acropora* spp. and “Other” corals were collected across all transects at Lagoon site 1 and 2 by hand on Jan 30 and Feb 12 2020. At each sampling time points the most visually ‘stressed’ (ranging from pale to completely bleached) corals were collected. 15 fragments from each group (*Acropora* spp. or “Other”) were collected at the study site and directly frozen in WhirlPak[®] bags at -80 °C. Tissue was removed from the skeleton using an airpik and compressed air from diving tanks. Tissue was blown into a zip-lock bag with 50ml of 0.45 µ filtered seawater. The algal pellet was washed three times (centrifuged at 3856 x g, 4 °C for 5 minutes) to remove mucous and coral tissue, before being frozen at -20 °C for later analysis. The pellet was suspended in 10 ml of filtered sea water and aliquots

were counted in triplicate using an improved Neubauer haemocytometer. Counts were normalized to fragment surface area using the wax method (Stimson and Kinzie III, 1991).

2.4 Lagoon Community Metabolism Measurements

Rates of daytime net ecosystem production (NEP; $\text{mmol O}_2 \text{ m}^{-2} \text{ h}^{-1}$) and net ecosystem calcification (NEC; $\text{mmol CaCO}_3 \text{ m}^{-2} \text{ h}^{-1}$) were estimated daily (tides and full sunlight permitting) over the course of 20 d (Jan 22 to Feb 12 2020) along the six transects. To estimate rates of NEP and NEC, changes in dissolved oxygen (DO) and total alkalinity (A_T) were measured, respectively, during a three-hour window around low tide and peak sunlight using both the slack-water and flow-respirometry (Eulerian) approach. Because differences in sunlight are a major driver in NEP variability, measurements were refined to days of full sunlight and low tides coinciding with near mid-day (11:00 – 15:00). Flow speeds across the transect were measured with an acoustic doppler velocimeter (ADV; Sontek [cm s^{-1}]) recording data at 15-min intervals. This ADV was placed at the end of the middle transect (Figure 1). Depth varied between 0.1 – 1m and was measured concurrently with water sample collections at each location. Depth was also measured at peak low tide at 5m intervals along each transect ($n = 120$ site-1) to ensure that sample location depths adequately represented the entirety of the transect.

Salinity (psu) and dissolved oxygen (DO: mg L^{-1}) was measured with a Hanna HI98194 multimeter and DO was converted to $\mu\text{mol kg}^{-1}$ using seawater density. DO probe calibration was performed weekly using a two-point calibration at 0 % (sodium thiosulfate) and 100 % saturated seawater equilibrated with the atmosphere. Samples for A_T were collected in 60 ml sample polycarbonate sample bottles, preserved with saturated Mercuric Chloride according to CO_2 best practices (Dickson, 2007), and sealed with a screw top lid and parafilm. Seawater A_T was analysed by potentiometric titration using a Metrohm 848 Titrino plus automatic titrator (~ 40 ml of seawater per sample) in duplicates (SD uncertainty $< 2 \mu\text{mol kg}^{-1}$). Overall analytical uncertainty for A_T (SD = $\pm 2.4 \mu\text{mol kg}^{-1}$) measurements was estimated from repeated measurements of certified reference materials from the Scripps Institute of Oceanography (CRM; Batch 161).

2.4.1 Eulerian Approach

Flow metabolism transects were established along a reef area previously characterised as degraded, where there is less than 10 % coral cover (Roelfsema et al., 2018). The flow-respirometry (i.e., Eulerian approach) measurements were conducted within two designated reef areas (100 m x 200 m; 0.02 km²) which significantly differed in coral cover. The defined study area was determined based on the necessary transect length to achieve measurable differences in seawater dissolved oxygen ($\Delta DO = \pm 4 - 7 \text{ mg L}^{-1}$) between upstream and downstream locations ($\sim 200 \text{ m}$; Langdon et al., 2010).

Repeated deployments of fluorescein dye packets across the research zone at differing tidal periods determined a specific 400 m x 100 m area of the reef where flow was unidirectional from east to west during a period spanning from 2 hours before to 1 hour after peak low tide (3 hours total). Outside of this period, the reef lagoon was no longer physically separated from the open ocean, flow became multidirectional, and the defined lagoon area became too deep and diluted with open ocean water to measure significant changes in seawater chemistry. The 400 m x 100 m area was then designated as two,. The spread of the dye path varied $\pm 25 \text{ m}$ in a north/south direction and triplicate 200 m transects were spaced 50 m apart in parallel at each site so that NEC and NEP were averaged across the three downstream locations, representing all potential water flow paths of the overall study site area. A flow meter was rotated between downstream water sample collection locations on ($n = 3 \text{ sampling location}^{-1}$) and determined continued placement of the one available ADV at the middle downstream location was adequate to represent flow speed across all three transects.. Within each area, three 200m transects were established in parallel, 50 m distance from one another (Fig. 1). Water samples were collected as close in time as possible at these fixed upstream and downstream locations ($n = 3 \text{ area}^{-1}$) at peak low tide while lagoon currents were unidirectional, running east to west.

$$\text{Equation 1: } NEP = \frac{3600}{100} \times \frac{\Delta DO \times \rho \times u \times d}{l}$$

$$\text{Equation 2: } NEC = \frac{3600}{100} \times \frac{0.5 \times \Delta TA \times \rho \times u \times d}{l}$$

The Eulerian approach requires the following measurements: The change in DO and A_T (ΔDO and ΔA_T ; mmol kg⁻¹), the mean seawater density (ρ ; kg m⁻³), the mean current speed (cm s⁻¹), the mean depth over the transect (d ; meters), and the length of the transect (l ; meters). For specific details on the arrangement of the equations above, including the 3600/100 parameter (to convert cm s⁻¹ to m h⁻¹), please refer to Langdon et al., (2010).

2.4.2 Slack Water Approach

The slack-water approach was used to estimate rates of NEP and NEC over a relatively larger area of reef (~ 0.3 km²) during a period of three hours around low tide. This period was chosen based on initial observations of current speed and direction which aligned with previous slack-water estimates on this specific area of the Heron lagoon (Stoltenberg et al., 2020). Starting two hours before peak low tide, the lagoon becomes separated from the open ocean and the current begins flowing unidirectionally toward the lagoon outlet to the west. This unidirectional flow behaviour continues until roughly 2 hours after peak low tide, at which time the flow begins to reverse as the tide fills back in over the reef crest. To avoid dilution with the open ocean and changing current vector directions confounding residence time estimates, water samples were collected from the same three locations ($n = 3$ day⁻¹) two hours before peak low tide and one hour following.

$$\text{Equation 1: } NEP = \frac{\Delta DO \times \rho \times d}{\Delta t}$$

$$\text{Equation 2: } NEC = \frac{0.5 \times \Delta A_T \times \rho \times d}{\Delta t}$$

The slack-water approach requires the following measurements: The change in DO and A_T (ΔDO and ΔA_T ; mmol kg⁻¹), the mean seawater density (ρ ; kg m⁻³), mean depth over the transect (d ; meters), and

time between sampling (Δt ; hours). Given the time between samples (~ 3 h) and mean current speeds (~ 20 cm s⁻¹), these measurements represent a transect length of roughly 2.5 – 3km of reef.

2.4.3 Approach Comparison

Both approaches to estimate NEP and NEC provide limitations and advantages with respect to each other (see Langdon et al., 2010). In the Eulerian approach, the exact benthic area contributing to measured changes in seawater chemistry is known and its constituents can be quantified and related to the calculated rates of benthic metabolism. This approach, however, measures change in alkalinity over a relatively smaller area and time-period. Resulting fluxes in A_T ($\pm 30 - 60$ $\mu\text{mol kg}^{-1}$) and DO ($\pm 20 - 50$ $\mu\text{mol kg}^{-1}$) are relatively small compared to the slack-water approach, thereby providing less confidence in calculated rates of benthic metabolism.

In contrast, the slack-water approach benefits from the relatively large changes in total alkalinity (A_T : $\pm 100 - 200$ $\mu\text{mol kg}^{-1}$) and dissolved oxygen (DO: $\pm 80 - 150$ $\mu\text{mol kg}^{-1}$), which provides more confidence in A_T anomaly calculations and represent a large area of the reef flat relative to this study's flow-respirometry estimates. This approach, however, lacks specificity of the exact area of reef affecting changes in chemistry and DO fluxes are more vulnerable to gas exchange anomalies. As such, relating metabolic rates to the benthic community provides uncertainties given daily changes in mean current speed and, subsequently, the area of benthos reflected in the A_T and DO anomaly.

Overall, the combination of both approaches can work in tandem to compensate for their respective weaknesses. However, neither approach can accommodate dilution with the open ocean and generally need to be conducted in full sunlight or darkness so that community metabolism does not transition between autotrophy and heterotrophy in the middle of the measurements. For this reason, community metabolism estimates were paused from Jan 27 – Feb 2 when peak low tide occurred around dawn and dusk and changes in DO and A_T were negligible.

2.4.4 Air-Sea Gas Exchange Corrections

NEP estimates were corrected for the air-sea gas exchange (F_{O_2}) of oxygen using the gas-transfer velocity relationships outlined by Wanninkhof (1992) and Wanninkhof et al., (2009). F_{O_2} was calculated with the following equation.

$$F_{O_2} = k K_0 (fO_{2_{water}} - fO_{2_{air}})$$

where k is the gas transfer velocity (calculated using and averaged daily wind speed from BOM data), K_0 is the gas transfer coefficient, $fO_{2_{water}}$ is the concentration of seawater dissolved oxygen (mg L^{-1}) at the time of the downstream measurement, $fO_{2_{air}}$ (mg L^{-1}) was assumed to be 100 % saturation at the air temperature over the 3-h measurement period ($\sim 8.10 \text{ mg L}^{-1}$).

2.4.5 Statistical Analyses

All statistical analyses were performed with the SPSS statistics software (SPSS Inc. 2013 Version 26.0). To compare measured differences in benthic cover (percent coral, percent algae, percent bleached coral tissue, sediment overgrowth) and community metabolism (NEP and NEC) between triplicate transects, measurement days ($n = 12$), and Lagoon sites (Lagoon site 1, Lagoon site 2, and Slack Water), a one-way analysis of variance (ANOVA) model was used in which transect, day, or site was a fixed effect and measured values for percent cover, NEP, and NEC were treated as the response variable. Results for percent cover compared among triplicate transects and Lagoon sites are displayed in Tables S1 and S2, respectively. Before community metabolism measurements were compared, assumptions of normality and equality of variance were evaluated with a Shapiro Wilk test (Table S4). Results for community metabolism compared among triplicate transects, measurement days, and Lagoon sites are displayed in Tables S5, S6, and S7, respectively. A Tukey HSD post-hoc test was used to perform pairwise comparisons for measured NEC between Lagoon site 1, Lagoon site 2, and the slack-water approach (Table S7). To explore relationships between NEC as a function of NEP, Model II regression techniques were used to test for significant linear relationships (cutoff value

292 $p < 0.1$) and an ANCOVA was used to test for differences in NEC vs. NEP slope categorized by
293 Lagoon site (Lagoon site 1 and Lagoon site 2).

294 3. Results

295 3.1 Lagoon Community Assemblage

296 Across the whole study area (Lagoon site 1 and Lagoon site 2 combined), the benthic community was
297 predominately covered by sediment ($59 \pm 7\%$) and fleshy algae ($25 \pm 6\%$). Coral cover ($5 \pm 3\%$) was
298 slightly higher relative to other recorded sessile calcifiers ($4 \pm 1\%$) and carbonate rubble covered in
299 coralline algae ($5 \pm 2\%$). Algae was the dominant benthic organism in both Lagoon site 1 ($28 \pm 4\%$)
300 and Lagoon site 2 ($22 \pm 4\%$) and cover was significantly higher at Lagoon site 1 ($p = 0.011$) (Table
301 1). Lagoon site 2 exhibited a significantly higher coral coverage ($8 \pm 3\%$) relative to Lagoon site 1 (3
302 $\pm 2\%$) ($p = 0.001$), the majority of which were *A. aspera*, *A. millepora*, and *M. digitata*. A description
303 of the mobile and sessile invertebrate diversity is described in Fig. 2 and the supplemental information
304 (S.4). A full list of observed invertebrates and accompanying photos can be found at
305 <https://www.inaturalist.org/projects/heron-island-survey-corals-inverts-and-algae>.

306 Overall, we found 25 coral species in the lagoonal reef study area, 22 of which were hard corals and
307 three soft corals (Fig. 2; Table S8). Thirteen algae morphospecies were observed, with one identified
308 as species *Valonia ventricosa* and the rest unidentified. Across all other invertebrate taxa, 19 species
309 of echinoderms, bivalves, and polychaetes, and 24 species of crustaceans and gastropods were
310 observed. Of the 43 non-coral invertebrate species, 15 were associated with colonies of *Pocillopora*
311 corals. Sea cucumbers (e.g., *Holothuria* spp., *Stichopus* spp.) were the dominant mobile invertebrate,
312 the Lollyfish sea cucumber (*Holothuria atra*) was the most common across both Lagoon sites ($1.2 \pm$
313 0.2 individuals m^{-2}). Second in abundance was the Hermann's Sea Cucumber (*Stichopus hermanni*)
314 (0.4 ± 0.1 individuals m^{-2}). Other notable invertebrates included Linckia sea stars (*Linckia guildingia*,
315 *Linckia laevigata*) and white-speckled sea hares (*Aplysia argus*) (all found in abundances < 0.1

316 individuals m⁻²). The largest mobile invertebrates observed were Bailer Shell snails (*Melo amphora*)
317 at 30 cm in length and white-spotted hermit crabs (*Dardanus megistos*) occupying Bailer shells (< 0.1
318 individuals m⁻²).

319 Our observations included 8 species with a conservation status of near threatened or higher, including
320 the small giant clam *Tridacna maxima*, Herrmann's sea cucumber (*Stichopus herrmanni*), and 6 coral
321 species (*Porites attenuata*, *Acropora secale*, *Isopora palifera*, *Stylophora pistillata*, *Favites halicora*,
322 *Favites rotundata*). Notably, our observation of the aglajid slug *Tubulophilinopsis gardineri* is one of
323 just 5 from Heron Island, representing the southernmost limit of its eastern coast distribution. We also
324 observed an undescribed nudibranch species, a yellow-brown *Gymnodoris* (Figure 5). A complete list
325 of all species described can be found in the Supplemental Material (Table S8).

326 **3.2 Lagoon Light and Temperature**

327 Temperature across the Lagoon site 1 exhibited a mean value of 28.6 ± 1.5 °C and varied between a
328 minimum of 25.8 °C and a maximum of 34.8 °C (Table 2). Light at Lagoon site 1 exhibited a mean
329 value of 328 ± 247 $\mu\text{mol quanta m}^{-2} \text{ s}^{-1}$ and maximum values of $1001 \mu\text{mol quanta m}^{-2} \text{ s}^{-1}$ (Fig. 1).
330 Temperature across Lagoon site 2 exhibited a mean value of 28.6 ± 1.5 °C and varied between a
331 minimum of 25.9 °C and a maximum of 34.6 °C. Light at Lagoon site 2 exhibited a mean value of 336
332 $\pm 254 \mu\text{mol quanta m}^{-2} \text{ s}^{-1}$ and maximum values of $969 \mu\text{mol quanta m}^{-2} \text{ s}^{-1}$.

333 Satellite monitoring data (5 km pixel resolution; NOAA Coral Reef Watch) indicated the accumulation
334 of heat stress beginning on Feb 1 2020. Lagoon temperatures peaked three days following on Feb 4th
335 (Fig. 1) at which time the first signs of coral bleaching were anecdotally observed within the study
336 area and on other areas of the Heron lagoon. Over the course of the study period a total of 3.59 DHWs
337 were accumulated. In the periods before and after the accumulation of heat stress (Feb 1st 2020),
338 Lagoon site 1 mean temperatures were 28.1 ± 1.4 °C and 29.0 ± 1.5 °C, respectively, and Lagoon site

339 2 mean temperatures were 28.0 ± 1.3 °C and 29.1 ± 1.5 °C, respectively. Further details on recorded
340 light and temperature data can be found in the supplemental information (S.5).

341 3.3 Lagoon Community Bleaching Extent

342 Dark-adapted yield was 0.662 ± 0.010 for *Acropora* spp. fragments and 0.576 ± 0.020 for “Other”
343 fragments (mean \pm SE, n = 35) on Feb 4th. On Feb 9th, yield declined 35 % for *Acropora* spp. to
344 0.430 ± 0.014 (n = 15) and 25 % for “Other” fragments to 0.434 ± 0.018 (n = 20). Symbiodiniaceae
345 densities were $0.976 \pm 0.135 \times 10^6$ cm⁻² for *Acropora* spp. (n = 15) and $0.507 \pm 0.160 \times 10^6$ cm⁻² for
346 “Other” fragments (n = 10) on Jan 30th. On Feb 12th, *Acropora* spp. densities had declined by 48 % to
347 $0.504 \pm 0.0849 \times 10^6$ cm⁻² (n = 15) and by 18 % for “Other” fragments to $0.414 \pm 0.094 \times 10^6$ cm⁻² (n
348 = 15) (Fig. 3).

349 Altogether, the percentage of coral tissue exhibiting bleaching increased from 0 % to 60 ± 11 % over
350 the course of the three photo-quadrat survey efforts (Table 3; Fig. S.1). Reef sediment was found to
351 exhibit increased growth of green and red microbial biofilms, which grew in cover from 2 ± 1 % to 12
352 ± 4 %. Coral bleaching observed during the study period was confirmed by PAM fluorometry (dark
353 adapted yield; Fv/Fm) and Symbiodiniaceae densities (cells $\times 10^6$ cm⁻²) measured during observed
354 bleaching (S.6).

355 3.4 Lagoon Community Metabolism

356 The mean \pm SD value of NEP and NEC at Lagoon site 1 and Lagoon site 2 (pooled together across
357 triplicate transects and measurement days [n = 36]) is displayed in Table 4 and Fig. 3 and separated by
358 the pre-bleaching (Jan 22nd to Feb 1st 2020) and bleaching period (Feb 2nd to Feb 10th 2020). Mean
359 daytime net ecosystem production (NEP), averaged across all days and sites, was 39.4 ± 12.2 mmol
360 O₂ m⁻² h⁻¹. NEP did not significantly differ across triplicate transects within Lagoon site 1 (p = 0.471)
361 or Lagoon site 2 (p = 0.917), so these data were pooled together to represent the overall community
362 NEP of each site (Fig. 3). The measured NEP throughout the study period was highly variable and did

not significantly differ over time ($n = 12$) at either Lagoon site 1 ($p = 0.181$) (lowest coral cover site) or Lagoon site 2 ($p = 0.099$) (highest coral cover site). NEP did not significantly differ between Lagoon site 1 and Lagoon site 2 ($p = 0.067$). NEP values were not included for the slack-water approach given the large source of error in air-sea oxygen exchange.

Mean daytime NEC, averaged across all days and sites, was $12.2 \pm 4.5 \text{ mmol CaCO}_3 \text{ m}^{-2} \text{ h}^{-1}$. Measured rates of daytime NEC did not significantly differ across triplicate transects within Lagoon site 1 ($p = 0.471$), Lagoon site 2 ($p = 0.917$) or the slack water ($p = 0.581$), so these data were pooled together to represent the overall NEC of each area (Table 4). Measured NEC was also highly variable and did not significantly differ over time at Lagoon site 1 ($p = 0.506$), Lagoon site 2 ($p = 0.365$), and the slack water ($p = 0.073$). Estimated NEC in the slack-water approach was significantly lower compared to Eulerian estimates at Lagoon site 1 ($p = 0.010$) and Lagoon site 2 ($p = 0.001$); these two latter sites did not significantly differ ($p = 0.666$). Changes in NEC were significantly related to changes in NEP at both Lagoon site 1 ($r^2 = 0.32$; $p = 0.042$) and Lagoon site 2 ($r^2 = 0.28$; $p = 0.046$). Slope values for daytime NEC vs. NEP for Lagoon site 1 and 2 were 0.28 and 0.24, respectively (Fig. S.2).

To determine potential effects of bleaching on night-time dissolution and respiration, night-time estimates of NEC and NEP were conducted three times throughout the study near the dates of observed progressed bleaching (Jan 23rd, Feb 4, Feb 12th). However, A_T and DO changes were too small during the Lagoon site 1 and Lagoon site 2 Eulerian estimates, so night-time NEC could only be confidently calculated from slack-water estimates. We found mean slack-water nighttime NEC ($-3.1 \pm 1.1 \text{ mmol CaCO}_3 \text{ m}^{-2} \text{ h}^{-1}$) did not significantly differ across transects ($p = 0.617$) or over time ($p = 0.083$) within the current study.

4. Discussion

4.1 Community Metabolism Response to Bleaching

386 The southwestern lagoon area of Heron Island (southern Great Barrier Reef) is a community
387 characterised by low coral cover of approximately 5 – 8 %. Within this reef area, the predominant
388 benthic cover was unpalatable algae (approximately 21 %), dominated by the two genera *Laurencia*
389 spp. and *Lobophora* spp., consistent with that of a degraded coral habitat (Hughes et al., 1999). Prior
390 surveys of the benthic cover in this area of the Heron Island lagoon (Scientific Zone) have also
391 estimated relatively low coral cover (0 - 10 %; Roelfsema et al., 2018).

392 Accumulation of heat stress in the lagoon over the study period resulted in 3.59 DHWs as *in-situ* mean
393 temperature was elevated from ~ 28.0 °C to ~ 29.1 °C (+1.1 °C). Over this period, we found that
394 approximately 60 % of corals present within both Lagoon sites 1 and 2 exhibited bleaching. These
395 bleaching observations were corroborated by both photosynthetic yields and Symbiodiniaceae
396 densities of all corals sampled. Photosynthetic yields recorded on Feb 4th 2020 in both the *Acropora*
397 spp. and “other” category were barely above values considered “healthy” (0.5 [Gierz et al., 2020]) and,
398 by Feb 9th 2020, exhibited symbiont loss with values below 0.5 (Acro = 0.43 ± 0.01 ; Other = Acro =
399 0.43 ± 0.01). Mean Symbiodiniaceae densities across both time points for the *Acropora* spp. ($0.74 \pm$
400 $0.11 \times 10^6 \text{ cm}^{-2}$) and “other” corals ($0.46 \pm 0.13 \times 10^6 \text{ cm}^{-2}$) were also below normally healthy values
401 previously recorded in both *Acropora* spp. ($1-2 \times 10^6 \text{ cm}^{-2}$ [Gierz et al., 2020]) and corals in the
402 “Other” category (e.g., *Montipora digitata*; $2-3 \times 10^6 \text{ cm}^{-2}$ [Klueter et al., 2006]) collected from the
403 Heron Island reef flat.

404 Despite the ongoing reef-wide bleaching event and measured decline in coral endosymbiont densities,
405 we find that NEP and NEC at both Lagoon sites did not significantly differ from estimates during the
406 pre-bleaching period or prior estimates on other Great Barrier Reef lagoon communities of similar
407 coral cover (e.g., $10 - 20 \text{ mmol CaCO}_3 \text{ m}^{-2} \text{ h}^{-1}$: Albright et al., 2015; Pisapia et al., 2019; Stoltenberg
408 et al., 2021). The lack of a bleaching effect was also mirrored in the slack water NEP and NEC data,
409 which represented a much larger cross section of the lagoon community (~ 2 – 3 km transects), where
410 bleaching was also observed (but not quantified during this study period). Importantly, these trends

differ from those observed by Courtney et al., (2018) during a 2015 bleaching event in Kaneohe Bay, Hawai'i (~ 10 % total cover), where a similar ~ 1 °C increase in mean reef temperature resulted in bleaching of 46 % of the coral community and both NEP and NEC were driven to zero. However, our results support those of Kayanne et al., (2005), where NEC and NEP remained relatively constant during a bleaching event (29 °C; 51 % bleached) in September of 1998 at Shiraho reef in Japan (5 – 7 % total coral cover). The critical difference between these studies is likely due to a threshold in total coral cover, where bleaching is less impactful on NEC when coral is not the dominant calcifying organism relative to the other calcifying constituents (sediments, rubble, calcifying algae, and other sessile or mobile gastropods and echinoderms) which are also known to contribute to the total reef carbonate budget and, in some cases, exhibit positive temperature-calcification relationships (Cornwall et al., 2019).

4.2 Estimated Organism Contribution to NEC at Elevated Temperatures

Importantly, if we consider that rubble observed in the Lagoon sites 1 and 2 (approximate cover of 4 %) was predominately covered in crustose coralline algae (CCA) and combine these with the other sessile calcifiers observed (which were predominantly *Halimeda* spp.; 3 % cover), then hermatypic corals were not the dominant reef calcifier. Further, if 60 % of the total coral cover was calcifying roughly 60 % slower due to bleaching (D'Olivo & McCulloch, 2017), this would imply that active calcifying coral cover was likely reduced to only 2 – 4 %. This adjusted 'calcifying percent coral cover' is minor compared to the sum of all other benthic constituents which were actively calcifying regardless of the SST conditions (Sediment + CCA + *Halimeda* = 72 %).

One possible explanation for the lack of any observed changes in NEC could be due to the simultaneous thermal enhancement of calcification in other benthic members when the reef seawater was warmed from 28.0 °C to 29.1 °C. To investigate the relative contribution to overall NEC from the assemblage of benthic calcifiers at these respective temperatures, we created an equation based on reported rates in the literature at 28.0 °C and 29.1 °C (Equation 1) where the summed community-level calcification

rate (NEC) at the respective temperature (T) is equal to the sum of the described calcification rates for each benthic organism category (Net Organism Calcification: NOC) multiplied by the recorded cover (Cover) across Lagoon sites 1 and 2 at that temperature (T).

$$\text{Equation 1 : } NEC_T = \sum (NOC_T \times Cover_T)$$

To estimate the potential effect of a +1.1 °C change in seawater temperature on coral calcification for corals observed within the lagoon study sites the following aquaria manipulation studies were reviewed: Edmunds, 2005; Anthony et al., 2008; Cantin et al., 2010; Comeau et al., 2013, 2016; and the following meta-analysis and modeling studies were reviewed: Lough and Barnes, 2000; McNeil et al., 2004; Evenhuis et al., 2015; Kornder et al., 2018; Bove et al., 2020. Together, these studies suggest mean calcification rates across coral genera most common to the Heron reef flat (*Acropora* spp., *Montipora* spp., *Porites* spp., *Pocillopora* spp.) at 28.0 °C ($4.53 \pm 2.31 \text{ mmol CaCO}_3 \text{ m}^{-2} \text{ h}^{-1}$) increase by approximately 22 % when warmed to a temperature of 29.1 °C. It is important to note this % increase is highly variable and species specific, so numbers used here are simply for the purpose of discussion. In comparison, calcification by crustose coralline algae (CCA), which is the next most studied organism (see meta-analysis by Cornwall et al., (2019)), has not exhibited changes until temperatures are as high as 5 °C above ambient temperatures. Therefore, no change was estimated for mean reported rates ($0.36 \pm 0.09 \text{ mmol CaCO}_3 \text{ m}^{-2} \text{ h}^{-1}$) for commonly studied CCA species (*Lithophyllum kotschyannum* and *Hydrolithon onkodes*).

Responses in calcification to warming for Halimeda algae are equivocal (Campbell et al., 2016; Wei et al., 2020). If constrained to species commonly identified on the Great Barrier Reef (such as *H. opuntia* and *H. cylindracea*; Aims, 2020) then it can be expected that increasing temperatures will increase rates of calcification up to temperatures of 30 °C, above which they bleach and exhibit a negative calcification response. As such, narrowed within the ranges observed during this study, calcification rates of Halimeda ($3.33 \pm 2.29 \text{ mmol CaCO}_3 \text{ m}^{-2} \text{ h}^{-1}$) are estimated to increase by

approximately 7.9 % in response to warming from 28.0 °C to 29.1 °C. Calcification responses to warming in carbonate sediments are overall the least studied of the benthic categories in this study, but potentially the most significant given the dominant cover of sediment. A study within the Heron Island lagoon indicates daytime sediment calcification at 28 °C ($1.41 \pm 0.29 \text{ mmol CaCO}_3 \text{ m}^{-2} \text{ h}^{-1}$) would increase ~ 9 % when seawater is warmed to 29.1 °C (Lantz et al., 2017).

When these trends are summed together with the expected 60 % decline in calcification for the proportion of coral that was bleached, a collective 9.8 % decline in NEC can be expected (Fig. 4). However, when each category is adjusted for the percent cover observed at the end of the study at 29.1 °C across both Lagoon sites, the total change in NEC increases by ~ 0.8 %. This is largely owed to positive trends in the calcification of other benthic community members and provides an explanation why no significant differences were observed in NEC during reef-wide coral bleaching. These estimates illustrate how the decline in coral calcification may be overshadowed by thermal acceleration in calcification in ahermatypic benthic calcifiers. Our findings highlight the need to better adjust how NEC is applied as a metric for community function during bleaching events, as these data suggest warming may create a divergence between estimated daytime NEC and actual reef growth on future degraded reef ecosystems.

4.3 Future Considerations

Our study highlights three considerations which may affect NEC which we suggest need to be further investigated to resolve monitoring issues for degraded coral reef communities. Firstly, the impact of night-time dissolution on overall 24-h NEC. Estimates of NEC at night ($n = 3$) in the current study did not exhibit a response to bleaching, but a higher frequency is needed. Courtney et al., (2018) hypothesized that the dissolution signal was a major driver of the net 24-h zero NEC signal during bleaching. These findings were more recently corroborated at the organism level by Orte et al. (2021), where algal turfs on dead coral calcified at the same rate as coral during the day but transitioned to net dissolving at night. This is supported by calcification responses to warming in the sediment, the most

dominant benthic member in this study, where warming-driven daytime increases in NEC were largely overshadowed by night-time increases in dissolution (Lantz et al., 2017) and the sediments transitioned to net dissolving over the full 24 h. These results suggest that future studies need include nighttime measurements of NEC and NOC but also highlights the limitation of flow-metabolism approaches as a representation of reef health given that not all reefs are easily accessible at night for such measurements.

Secondly the longer-term changes in NEC (when bleached coral eventually dies or the thermal benefits to other calcifiers expire) needs to be investigated if we are to accurately estimate community function in future reef scenarios. In the current study we did not monitor the response in NEC following the 2020 bleaching event when a return to 28 °C or lower would likely reduce the thermal benefits to daytime calcification in the sediment, rubble, live coral, and *Halimeda* algae which potentially masked the minimized contribution from bleached coral. Under these assumptions, a 7.6 % decline in NEC would be expected when temperatures return to 28 °C. Additionally, if we assume the bleached coral eventually dies, and a 60 % reduction to calcification increases to a 100 % reduction, then community NEC would in theory exhibit a total 13.1 % decline. These post-bleaching estimates may explain the differences between this study and post-bleaching NEC estimates reported similarly degraded reef transects at Lizard Island, Australia (3 % coral cover) by McMahon et al., 2019, where post-bleaching NEC in 2016 declined by 40 – 46 % relative to pre-bleaching estimates in 2008 when coral cover was higher (~ 8 % coral).

Finally, the indirect feedbacks on NOC from non-calcifying community members (e.g., algae) and the carbonate substrate they occupy also needs to be considered to predict future reef growth (Orte et al., 2021). The sum of adjusted NOC (Fig. 4; 1.30 mmol CaCO₃ m⁻² h⁻¹) only explains 10.6 % of the measured NEC (12.3 mmol CaCO₃ m⁻² h⁻¹). Such discrepancies may be explained the exclusion of the 21 % of space occupied by non-calcifying algae in the NOC summation exercise in Fig. 4. It is possible algae can provide positive feedback mechanisms to coral calcification through adjacent algal-driven

NEP (and subsequent modifications to the surrounding seawater carbonate chemistry; Gattuso et al., 1998; Unsworth et al., 2012) or the endolithic micro-calcifiers living inside the dead carbonate substrate colonized by algal communities (Orte et al., 2021). For example, endolithic microflora (Cyanophyta and Chlorophyta) living within carbonate rocks have been found to modify interstitial pH just beneath substrate surface to values as high as 8.5 (Reyes-Nivia et al., 2013), thereby creating localized zones supersaturated with aqueous Ca^{2+} and CO_3^{2-} ions (Krause et al. 2019) and promoting the inorganic precipitation of minerals such as brucite, micrite and dolomite. Critically, these microfloral communities are more diverse and abundant when living beneath turf algae compared to corals (Gutierrez-Isaza et al. 2015), are comparable in their productivity to overlying turf algae (Tribollet et al. 2006), and have been found to precipitate dolomite at an accelerated rate when seawater temperatures were increased from 28 °C to 30 °C (Diaz-Pulido et al. 2014). Taken together, this shows that these microfloral communities have the capacity to influence bulk seawater chemistry measurements particularly during coral bleaching events, where warm and well-lit conditions promote their growth. In addition to these microflora, various cryptic infaunal and endolithic macrofauna calcify to produce protective shells or burrows (e.g., Diaz-Castaneda et al., 2019) and may also be contributing to NEC signal measured during the bleaching event.

4.4 Conclusions

Ocean warming, and subsequent coral bleaching events, have already degraded coral reef ecosystems for over four decades and will continue to degrade coral reefs worldwide, reducing their capacity to provide critical habitat structure. While estimates of NEC via the alkalinity anomaly technique may be an appropriate benchmark of community function well after bleaching events have occurred and degradation to the coral community is fully realized, the results from this study highlight the shortcomings of using this approach to estimate daytime NEC when monitoring the effect of bleaching on reef accretion in real-time. These results, in conjunction with available literature on the importance of nighttime dissolution, suggest that flow-metabolism approaches to estimate community health may

535 be limited to reefs accessible at night (e.g., those near a research station or without navigational
536 hazards). Moreover, our study highlights that if coral cover continues to decline as predicted, NEC
537 may no longer be an appropriate proxy for reef accretion as the proportion of the NEC signal owed to
538 ahermatypic calcification increases. Additional estimates of NEC during bleaching events are urgently
539 needed to further explore the potential decoupling of positive NEC and reef growth. Concerningly, the
540 data herein suggest that NEC may begin to exhibit limitations as monitoring tool for reef growth when
541 coral becomes the minority benthic constituent.

542 **Author Contributions**

543 Coulson Lantz is responsible for study design, data collection and analysis, and writing. William
544 Leggat is responsible for study design, data analysis, and writing. Jessica Bergman is responsible for
545 data collection, analysis, and writing. Alexander Fordyce is responsible for data collection, analysis,
546 and writing. Charlotte Page is responsible for data collection, analysis, and writing. Thomas Mesaglio
547 is responsible for data collection and analysis, and writing. Tracy Ainsworth is responsible for study
548 design, data analysis, and writing.

549 **Acknowledgements**

550 This work was funded by the Australian Research Council DP 180103199. We thank the Heron Island
551 Research Station scientific staff for their support during research. We also thank all iNaturalist users
552 that helped identify the invertebrates photographed during this study, especially Joe Rowlett, Sean
553 Ono, Frédéric Ducarme and Pierre Mascar.

554 **Data availability statement**

555 Data is presently being submitted to PANGAEA data repository and a DOI will be provided upon
556 completion.

References

- Anon: Halimeda composition and biomass along the Great Barrier Reef | AIMS metadata | aims.gov.au, [online] Available from: <https://apps.aims.gov.au/metadata/view/7f7e70a0-c3db-472c-90d4-1ae243d8180b> (Accessed 1 September 2020), n.d.
- Anthony, K. R. N., Kline, D. I., Diaz-Pulido, G., Dove, S. and Hoegh-Guldberg, O.: Ocean acidification causes bleaching and productivity loss in coral reef builders, *Proc. Natl. Acad. Sci. U. S. A.*, 105(45), 17442–17446, doi:10.1073/pnas.0804478105, 2008.
- Albright, R., Benthuyssen, J., Cantin, N., Caldeira, K. and Anthony, K.: Coral reef metabolism and carbon chemistry dynamics of a coral reef flat, *Geophys. Res. Lett.*, 42(10), 3980–3988, doi:10.1002/2015GL063488, 2015.
- Bahr, K. D., Jokiel, P. L. and Rodgers, K. S.: Influence of solar irradiance on underwater temperature recorded by temperature loggers on coral reefs, *Limnol. Oceanogr. Methods*, 14(5), n/a-n/a, doi:10.1002/lom3.10093, 2016.
- Baird, A. H. and Marshall, P. A.: Mortality, growth and reproduction in scleractinian corals following bleaching on the Great Barrier Reef, *Mar. Ecol. Prog. Ser.*, 237, 133–141, doi:10.3354/meps237133, 2002.
- Bove, C. B., Umbanhowar, J. and Castillo, K. D.: Meta-Analysis Reveals Reduced Coral Calcification Under Projected Ocean Warming but Not Under Acidification Across the Caribbean Sea, *Front. Mar. Sci.*, 7, 127, doi:10.3389/fmars.2020.00127, 2020.
- Brown, J. H., Gillooly, J. F., Allen, A. P., Savage, V. M. and West, G. B.: Toward a metabolic theory of ecology, in *Ecology*, vol. 85, pp. 1771–1789, John Wiley & Sons, Ltd., 2004.
- Bruno, J. F. and Selig, E. R.: Regional decline of coral cover in the Indo-Pacific: Timing, extent, and subregional comparisons, edited by R. Freckleton, *PLoS One*, 2(8), e711, doi:10.1371/journal.pone.0000711, 2007.
- Campbell, J. E., Fisch, J., Langdon, C. and Paul, V. J.: Increased temperature mitigates the effects of ocean acidification in calcified green algae (*Halimeda* spp.), *Coral Reefs*, 35(1), 357–368, doi:10.1007/s00338-015-1377-9, 2016.
- Cantin, N. E., Cohen, A. L., Karnauskas, K. B., Tarrant, A. M. and McCorkle, D. C.: Ocean warming slows coral growth in the central Red Sea, *Science* (80-.), 329(5989), 322–325, doi:10.1126/science.1190182, 2010.
- Castillo, K. D., Ries, J. B., Bruno, J. F. and Westfield, I. T.: The reef-building coral *Sclerastrea siderea* exhibits parabolic responses to ocean acidification and warming, *Proc. R. Soc. B Biol. Sci.*, 281(1797), 1–9, doi:10.1098/rspb.2014.1856, 2014.
- Comeau, S., Edmunds, P. J., Spindel, N. B. and Carpenter, R. C.: The responses of eight coral reef calcifiers to increasing partial pressure of CO₂ do not exhibit a tipping point, *Limnol. Oceanogr.*, 58(1), 388–398, doi:10.4319/lo.2013.58.1.0388, 2013.
- Comeau, S., Carpenter, R. C., Lantz, C. A. and Edmunds, P. J.: Parameterization of the response of calcification to temperature and pCO₂ in the coral *Acropora pulchra* and the alga *Lithophyllum kotschyannum*, *Coral Reefs*, 35(3), 929–939, doi:10.1007/s00338-016-1425-0, 2016.
- Cornwall, C. E., Diaz-Pulido, G. and Comeau, S.: Impacts of ocean warming on coralline algae: Knowledge gaps and key recommendations for future research, *Front. Mar. Sci.*, 6(MAR), 186, doi:10.3389/fmars.2019.00186, 2019.

599 Courtney, T. A., De Carlo, E. H., Page, H. N., Bahr, K. D., Barro, A., Howins, N., Tabata, R., Terlouw,
600 G., Rodgers, K. S. and Andersson, A. J.: Recovery of reef-scale calcification following a bleaching
601 event in Kāneʻohe Bay, Hawaiʻi, *Limnol. Oceanogr. Lett.*, 3(1), 1–9, doi:10.1002/lol2.10056,
602 2018.

603 DeCarlo, T. M., Cohen, A. L., Wong, G. T. F., Shiah, F. K., Lentz, S. J., Davis, K. A., Shamberger, K.
604 E. F. and Lohmann, P.: Community production modulates coral reef pH and the sensitivity of
605 ecosystem calcification to ocean acidification, *J. Geophys. Res. Ocean.*, 122(1), 745–761,
606 doi:10.1002/2016JC012326, 2017.

607 Orte, M. R. de, Koweek, D. A., Cyronak, T., Takeshita, Y., Griffin, A., Wolfe, K., Szmant, A.,
608 Whitehead, R., Albright, R. and Caldeira, K.: Unexpected role of communities colonizing dead
609 coral substrate in the calcification of coral reefs, *Limnol. Oceanogr.*, 66(5), 1793–1803,
610 doi:10.1002/LNO.11722, 2021.

611 Díaz-Castañeda, V., Erin Cox, T., Gazeau, F., Fitzer, S., Delille, J., Alliouane, S. and Gattuso, J. P.:
612 Ocean acidification affects calcareous tube growth in adults and reared offspring of serpulid
613 polychaetes, *J. Exp. Biol.*, 222(13), doi:10.1242/jeb.196543, 2019.

614 Diaz-Pulido, G., McCook, L. J., Dove, S., Berkelmans, R., Roff, G., Kline, D. I., Weeks, S., Evans, R.
615 D., Williamson, D. H. and Hoegh-Guldberg, O.: Doom and Boom on a Resilient Reef: Climate
616 Change, Algal Overgrowth and Coral Recovery, edited by S. A. Sandin, *PLoS One*, 4(4), e5239,
617 doi:10.1371/journal.pone.0005239, 2009.

618 Diaz-Pulido, G., Nash, M. C., Anthony, K. R. N., Bender, D., Opdyke, B. N., Reyes-Nivia, C. and
619 Troitzsch, U.: Greenhouse conditions induce mineralogical changes and dolomite accumulation
620 in coralline algae on tropical reefs, *Nat. Commun.*, 5(1), 1–9, doi:10.1038/ncomms4310, 2014.

621 Dickson, A. G., Sabine, C. L. and Christian, J. R.: Guide to best practices for ocean CO₂
622 measurements, North Pacific Marine Science Organization., 2007.

623 Dove, S. G., Kline, D. I., Pantos, O., Angly, F. E., Tyson, G. W. and Hoegh-Guldberg, O.: Future reef
624 decalcification under a business-as-usual CO₂ emission scenario, *Proc. Natl. Acad. Sci. U. S. A.*,
625 110(38), 15342–15347, doi:10.1073/pnas.1302701110, 2013.

626 Edinger, E. N., Limmon, G. V., Jompa, J., Widjatmoko, W., Heikoop, J. M. and Risk, M. J.: Normal
627 coral growth rates on dying reefs: Are coral growth rates good indicators of reef health?, *Mar.*
628 *Pollut. Bull.*, 40(5), 404–425, doi:10.1016/S0025-326X(99)00237-4, 2000.

629 Edmunds, P. J.: The effect of sub-lethal increases in temperature on the growth and population
630 trajectories of three scleractinian corals on the southern Great Barrier Reef, *Oecologia*, 146(3),
631 350–364, doi:10.1007/s00442-005-0210-5, 2005.

632 Evenhuis, C., Lenton, A., Cantin, N. E. and Lough, J. M.: Modelling coral calcification accounting
633 for the impacts of coral bleaching and ocean acidification, *Biogeosciences*, 12(9), 2607–2630,
634 doi:10.5194/bg-12-2607-2015, 2015.

635 Eyre, B. D., Cyronak, T., Drupp, P., De Carlo, E. H., Sachs, J. P. and Andersson, A. J.: Coral reefs
636 will transition to net dissolving before end of century., *Science*, 359(6378), 908–911,
637 doi:10.1126/science.aao1118, 2018.

638 Gattuso, J. P., Frankignoulle, M., Bourge, I., Romaine, S. and Buddemeier, R. W.: Effect of calcium
639 carbonate saturation of seawater on coral calcification, *Glob. Planet. Change*, 18(1–2), 37–46,
640 doi:10.1016/S0921-8181(98)00035-6, 1998.

641 Gierz, S., Ainsworth, T. D. and Leggat, W.: Diverse symbiont bleaching responses are evident from
642 2-degree heating week bleaching conditions as thermal stress intensifies in coral, *Mar. Freshw.*
643 *Res.*, 71(9), 1149, doi:10.1071/MF19220, 2020.

644 Glynn, P. W.: Coral reef bleaching: ecological perspectives, *Coral Reefs*, 12(1), 1–17,
645 doi:10.1007/BF00303779, 1993.

646 Grigg, R.W., and Dollar, S.J. Natural and anthropogenic disturbance on coral reefs. *Coral Reefs*. Vol.
647 25, pp. 439–452. 1990.

648 Gutiérrez-Isaza, N., Espinoza-Avalos, J., León-Tejera, H. P. and González-Solís, D.: Endolithic
649 community composition of *Orbicella faveolata* (Scleractinia) underneath the interface between
650 coral tissue and turf algae, *Coral Reefs*, 34(2), 625–630, doi:10.1007/s00338-015-1276-0, 2015.

651 Harney, J. N. and Fletcher, C. H.: A Budget of Carbonate Framework and Sediment Production, Kailua
652 Bay, Oahu, Hawaii, *J. Sediment. Res.*, 73(6), 856–868, doi:10.1306/051503730856, 2007.

653 Heron, S. F., Maynard, J. A., Van Hooidek, R. and Eakin, C. M.: Warming Trends and Bleaching
654 Stress of the World’s Coral Reefs 1985-2012, *Sci. Rep.*, 6(1), 1–14, doi:10.1038/srep38402,
655 2016.

656 Hughes, T., Szmant, A. M., Steneck, R., Carpenter, R. and Miller, S.: Algal blooms on coral reefs:
657 What are the causes?, *Limnol. Oceanogr.*, 44(6), 1583–1586, doi:10.4319/lo.1999.44.6.1583,
658 1999.

659 Kayanne, H., Hata, H., Kudo, S., Yamano, H., Watanabe, A., Ikeda, Y., Nozaki, K., Kato, K., Negishi,
660 A. and Saito, H.: Seasonal and bleaching-induced changes in coral reef metabolism and CO₂ flux,
661 *Global Biogeochem. Cycles*, 19(3), 1–11, doi:10.1029/2004GB002400, 2005.

662 Klueter, A., Loh, W., Hoegh-Guldberg, O. and Dove, S.: Physiological and genetic properties of two
663 fluorescent colour morphs of the coral *Montipora digitata*, *Symbiosis*, 42(3), 123–134 [online]
664 Available from: <https://www.cabdirect.org/cabdirect/abstract/20073143496> (Accessed 23
665 September 2020), 2006.

666 Kornder, N. A., Riegl, B. M. and Figueiredo, J.: Thresholds and drivers of coral calcification
667 responses to climate change, *Glob. Chang. Biol.*, 24(11), 5084–5095, doi:10.1111/gcb.14431,
668 2018.

669 Krause, S., Liebetrau, V., Nehrke, G., Damm, T., Büsse, S., Leipe, T., Vogts, A., Gorb, S. N. and
670 Eisenhauer, A.: Endolithic Algae Affect Modern Coral Carbonate Morphology and Chemistry,
671 *Front. Earth Sci.*, 7, 304, doi:10.3389/feart.2019.00304, 2019.

672 Langdon, C., Gattuso, J.-P., Andersson, A., Océanologique, O. and Pierre, U.: Part 3 : Measurements
673 of CO₂ - sensitive processes 13 Measurements of calcification and dissolution of benthic
674 organisms and communities Part 3 : Measurements of CO₂ - sensitive processes, , 213–232,
675 2010.

676 Lantz, C. A., Schulz, K. G., Stoltenberg, L. and Eyre, B. D.: The short-term combined effects of
677 temperature and organic matter enrichment on permeable coral reef carbonate sediment
678 metabolism and dissolution, *Biogeosciences*, 14(23), 5377–5391, doi:10.5194/bg-14-5377-2017,
679 2017.

680 Liu, G., Strong, A. E., Skirving, W. J. and Arzayus, L. F.: Overview of NOAA Coral Reef Watch
681 Program’s near-real-time satellite global coral bleaching monitoring activities. [online] Available
682 from: <http://coralreefwatch.noaa.gov/>, 2006.

683 Lough, J. M. and Barnes, D. J.: Environmental controls on growth of the massive coral *Porites*, J.
684 Exp. Mar. Bio. Ecol., 245(2), 225–243, doi:10.1016/S0022-0981(99)00168-9, 2000.

685 McMahon, A., Santos, I. R., Schulz, K. G., Scott, A., Silverman, J., Davis, K. L. and Maher, D. T.:
686 Coral Reef Calcification and Production After the 2016 Bleaching Event at Lizard Island, Great
687 Barrier Reef, J. Geophys. Res. Ocean., 124(6), 4003–4016, doi:10.1029/2018JC014698, 2019.

688 McNeil, B. I., Matear, R. J. and Barnes, D. J.: Coral reef calcification and climate change: The effect
689 of ocean warming, Geophys. Res. Lett., 31(22), 1–4, doi:10.1029/2004GL021541, 2004.

690 Pisapia, C., Hochberg, E. J. and Carpenter, R.: Multi-Decadal Change in Reef-Scale Production and
691 Calcification Associated With Recent Disturbances on a Lizard Island Reef Flat, Front. Mar. Sci.,
692 6, 575, doi:10.3389/fmars.2019.00575, 2019.

693 Reyes-Nivia, C., Diaz-Pulido, G., Kline, D., Guldborg, O. H. and Dove, S.: Ocean acidification and
694 warming scenarios increase microbioerosion of coral skeletons, Glob. Chang. Biol., 19(6), 1919–
695 1929, doi:10.1111/gcb.12158, 2013.

696 Ries, J. B., Cohen, A. L. and McCorkle, D. C.: Marine calcifiers exhibit mixed responses to CO₂-
697 induced ocean acidification, Geology, 37(12), 1131–1134, doi:10.1130/G30210A.1, 2009.

698 Roelfsema, C., Kovacs, E., Ortiz, J. C., Wolff, N. H., Callaghan, D., Wettle, M., Ronan, M.,
699 Hamylton, S. M., Mumby, P. J. and Phinn, S.: Coral reef habitat mapping: A combination of
700 object-based image analysis and ecological modelling, Remote Sens. Environ., 208, 27–41,
701 doi:10.1016/j.rse.2018.02.005, 2018.

702 Rueden, C. T., Schindelin, J., Hiner, M. C., DeZonia, B. E., Walter, A. E., Arena, E. T. and Eliceiri,
703 K. W.: ImageJ2: ImageJ for the next generation of scientific image data, BMC Bioinformatics,
704 18(1), 1–26, doi:10.1186/s12859-017-1934-z, 2017.

705 Sully, S., Burkepille, D. E., Donovan, M. K., Hodgson, G. and van Woesik, R.: A global analysis of
706 coral bleaching over the past two decades, Nat. Commun., 10(1), 1–5, doi:10.1038/s41467-019-
707 09238-2, 2019.

708 Stoltenberg, L., Schulz, K. G., Lantz, C. A., Cyronak, T. and Eyre, B. D.: Late afternoon seasonal
709 transition to dissolution in a coral reef: An early warning of a net dissolving ecosystem?,
710 Geophys. Res. Lett., e2020GL090811, doi:10.1029/2020gl090811, 2021.

711 Stimson, J. and Kinzie, R. A.: The temporal pattern and rate of release of zooxanthellae from the reef
712 coral *Pocillopora damicornis* (Linnaeus) under nitrogen-enrichment and control conditions, J.
713 Exp. Mar. Bio. Ecol., 153(1), 63–74, doi:10.1016/S0022-0981(05)80006-1, 1991.

714 Tribollet, A., Langdon, C., Golubic, S. and Atkinson, M.: Endolithic microflora are major primary
715 producers in dead carbonate substrates of Hawaiian coral reefs, J. Phycol., 42(2), 292–303,
716 doi:10.1111/j.1529-8817.2006.00198.x, 2006.

717 Unsworth, R. K. F., Collier, C. J., Henderson, G. M. and McKenzie, L. J.: Tropical seagrass meadows
718 modify seawater carbon chemistry: Implications for coral reefs impacted by ocean acidification,
719 Environ. Res. Lett., 7(2), 9, doi:10.1088/1748-9326/7/2/024026, 2012.

720 Wanninkhof, R.: Relationship between wind speed and gas exchange over the ocean, J. Geophys.
721 Res., 97(C5), 7373–7382, doi:10.1029/92JC00188, 1992.

722 Wanninkhof, R., Asher, W. E., Ho, D. T., Sweeney, C. and McGillis, W. R.: Advances in
723 Quantifying Air-Sea Gas Exchange and Environmental Forcing, Ann. Rev. Mar. Sci., 1(1), 213–
724 244, doi:10.1146/annurev.marine.010908.163742, 2009.

- 725 Warner, M. E., Fitt, W. K. and Schmidt, G. W.: Damage to photosystem II in symbiotic dinoflagellates:
726 A determinant of coral bleaching, *Proc. Natl. Acad. Sci. U. S. A.*, 96(14), 8007–8012,
727 doi:10.1073/pnas.96.14.8007, 1999.
- 728 Wei, Z., Mo, J., Huang, R., Hu, Q., Long, C., Ding, D., Yang, F. and Long, L.: Physiological
729 performance of three calcifying green macroalgae *Halimeda* species in response to altered
730 seawater temperatures, *Acta Oceanol. Sin.*, 39(2), 89–100, doi:10.1007/s13131-019-1471-3, 2020.
- 731 Yvon-Durocher, G., Jones, J. I., Trimmer, M., Woodward, G. and Montoya, J. M.: Warming alters the
732 metabolic balance of ecosystems, *Philos. Trans. R. Soc. B Biol. Sci.*, 365(1549), 2117–2126,
733 doi:10.1098/rstb.2010.0038, 2010.

734 **Tables**

735 **Table 1:** Percent cover (Mean \pm SD) measured during point-contact and photo-quadrat surveys. Data
 736 for point contact surveys were pooled across triplicate transects and repeated survey efforts ($n = 6 \text{ site}^{-1}$)
 737 ¹⁾ within each Lagoon site area. Data for photo-quadrat surveys were pooled across triplicate transects
 738 and repeated survey efforts within each Lagoon site area ($n = 360 \text{ site}^{-1}$).

Category	Lagoon site 1		Lagoon site 2		Total
	Point Contact	Photo Quad	Point Contact	Photo Quad	Mean Cover
Hard Coral	$3 \pm 2 \%$	$3 \pm 2 \%$	$8 \pm 3 \%$	$9 \pm 3 \%$	6 %
Soft Coral	1 % <	1 % <	1 % <	1 % <	1 % <
Algae	$27 \pm 4 \%$	$18 \pm 5 \%$	$23 \pm 4 \%$	$16 \pm 4 \%$	21 %
Other Calcifier	$3 \pm 2 \%$	$2 \pm 2 \%$	$6 \pm 1 \%$	$2 \pm 2 \%$	3 %
Rubble	$4 \pm 3 \%$	$2 \pm 2 \%$	$5 \pm 3 \%$	$3 \pm 3 \%$	4 %
Sediment	$62 \pm 6 \%$	$74 \pm 7 \%$	$57 \pm 7 \%$	$69 \pm 6 \%$	65 %

739 **Table 2:** Mean values for physiochemical parameters measured at Lagoon site 1 and Lagoon site 2
740 over the course of the study. Temperature and light were logged continuously at 15-min intervals.
741 Temperature data are separated by the pre-bleaching period (Jan 22 – Feb 1 2020) and bleaching period
742 (Feb 2 – Feb 10 2020). Salinity was measured with each collected water sample ($n = 60 \text{ site}^{-1}$). Depth
743 was measured at peak low tide at 5m intervals along each transect ($n = 120 \text{ site}^{-1}$). The flow meter was
744 rotated between downstream water sample collection locations on each day of collection ($n = 5 \text{ site}^{-1}$).

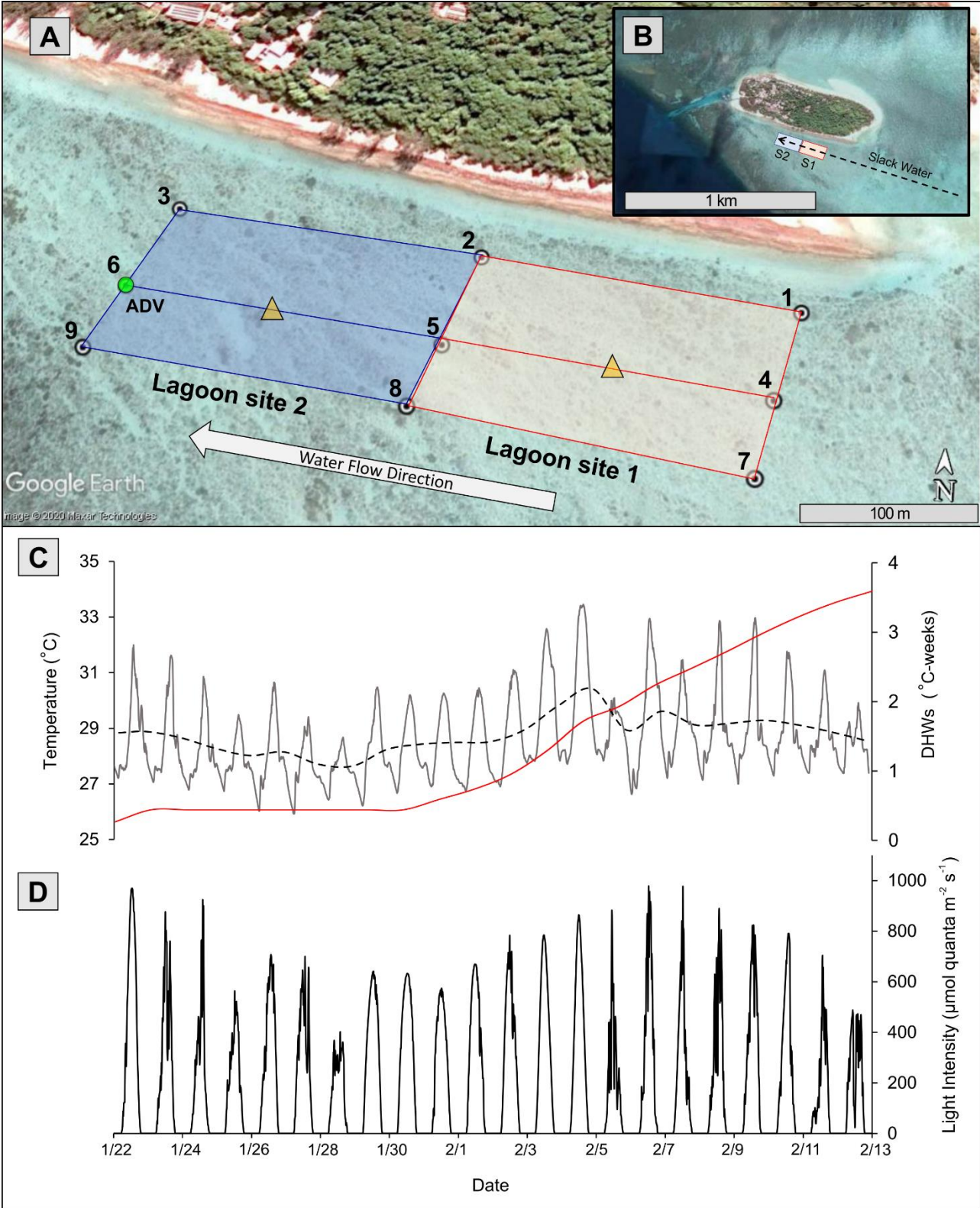
Parameter	Lagoon site 1	Lagoon site 2	Mean
Temperature ($^{\circ} \text{C}$) Pre-Bleaching	28.1 ± 1.3	28.0 ± 1.3	28.0 ± 1.3
Temperature ($^{\circ} \text{C}$) Bleaching	29.0 ± 1.5	29.1 ± 1.5	29.1 ± 1.5
Salinity (PSU)	35.6 ± 0.2	35.7 ± 0.2	35.7 ± 0.2
Light ($\mu\text{mol m}^{-2} \text{s}^{-1}$)	328 ± 247	336 ± 254	332 ± 251
Depth (cm)	37 ± 7	36 ± 6	37 ± 7
Flow (cm s^{-1})	21.6 ± 2.9	19.2 ± 3.8	20.4 ± 3.3

745 **Table 3:** Change in the relative percent area (Mean \pm SD) of coral tissue exhibiting paling or bleaching
746 (Bleached Coral Tissue) and relative percent area (Mean \pm SD) of sediment exhibiting overgrowth in
747 the form of visible cyanobacteria mats or Chlorophyta growth (Overgrowth on Sediment) over the
748 course of three different survey efforts. Data for each date are pooled across parallel transects within
749 each Lagoon site ($n = 120 \text{ site}^{-1}$).

	Study Site	Jan 24 2020	Feb 6 2020	Feb 12 2020
Bleached Coral Tissue	Lagoon site 1	0 \pm 0 %	16 \pm 3 %	55 \pm 8 %
	Lagoon site 2	0 \pm 0 %	24 \pm 6 %	65 \pm 10 %
Overgrowth On Sediment	Lagoon site 1	2 \pm 1 %	4 \pm 2 %	10 \pm 2 %
	Lagoon site 2	3 \pm 1 %	5 \pm 3 %	14 \pm 5 %

750 **Table 4:** Mean \pm SD values for daytime net ecosystem production (NEP; mmol O₂ m⁻² h⁻¹) and net
751 ecosystem calcification (NEC; mmol CaCO₃ m⁻² h⁻¹) for Lagoon site 1 and Lagoon site 2, where the
752 Eulerian approach was used (n = 12). NEC for the slack-water approach included for daytime (n = 11)
753 and night time (n = 3) estimates. Data are separated by the pre-bleaching period (Jan 22 – Feb 1 2020)
754 and bleaching period (Feb 2 – Feb 10 2020; n = 8). Nighttime rates for NEC are included NEP values
755 are not included for the slack-water approach given the large source of error in air-sea oxygen
756 exchange.

Approach	NEP (mmol O ₂ m ⁻² h ⁻¹)		NEC (mmol CaCO ₃ m ⁻² h ⁻¹)	
	Pre-Bleaching	Bleaching	Pre-Bleaching	Bleaching Period
Lagoon site 1	35.0 \pm 12.7	39.7 \pm 9.6	12.5 \pm 4.5	12.6 \pm 4.8
Lagoon site 2	44.4 \pm 13.6	38.7 \pm 13.8	13.3 \pm 5.7	12.3 \pm 5.4
Slack Water (day)			11.0 \pm 2.9	10.5 \pm 3.0
Slack Water (night)			- 2.8 \pm 0.7	- 3.4 \pm 1.3

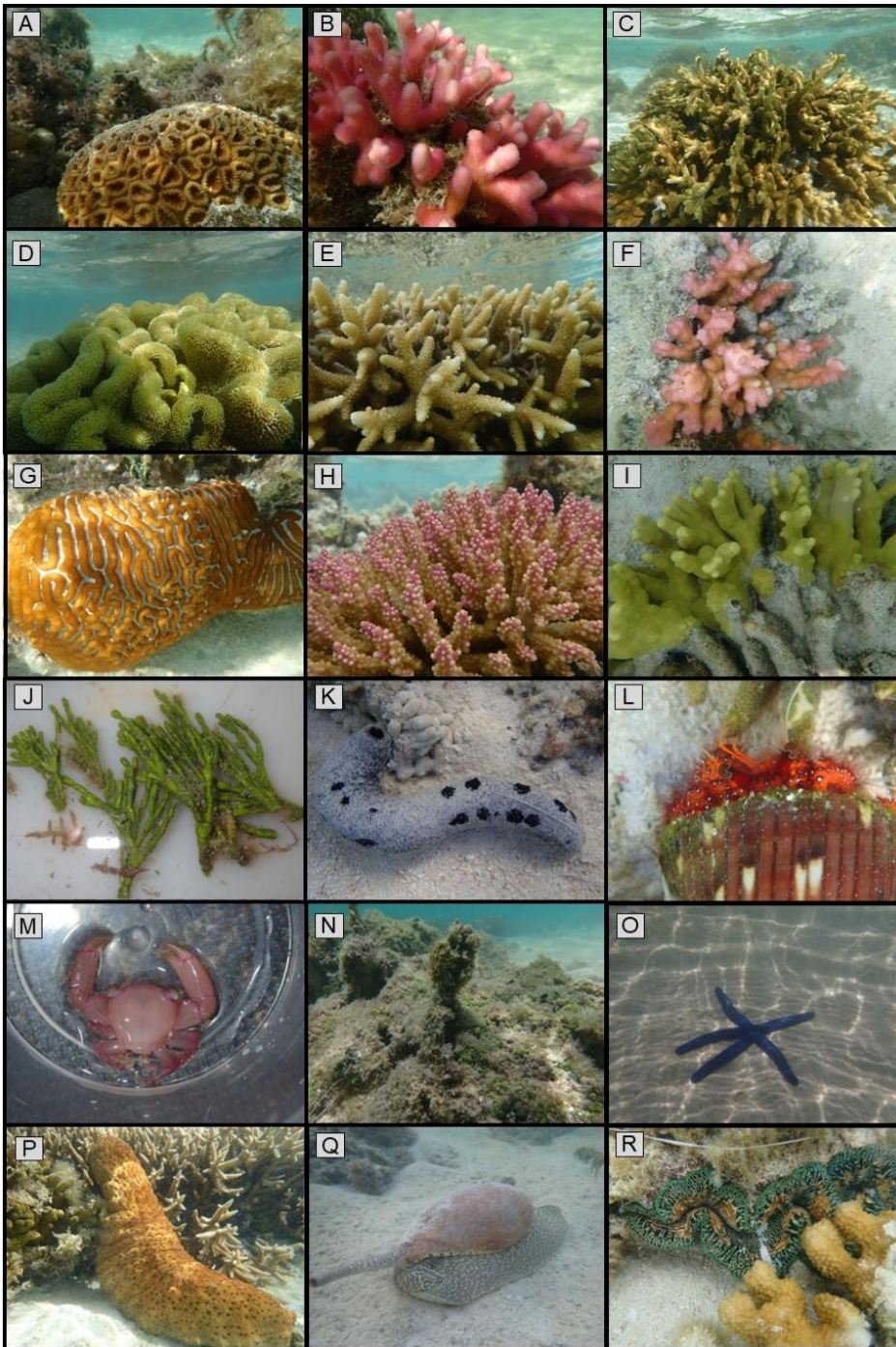


758

759 **Figure 1:** A) Study area (100 m scale) subdivided into Lagoon site 1 (red) and Lagoon site 2 (blue),.

760 White numbered circles (1 – 9) indicate of location water samples and temperature loggers. Yellow

761 triangles indicate location of light loggers. B) Study area (1 km scale) showing Lagoon site 1 (S1) and
762 Lagoon site 2 (S2) in relation to Heron Island and the larger slack-water area. C) In-situ lagoon
763 temperature ($^{\circ}\text{C}$) averaged across both sites measured by temperature loggers. Black dashed line
764 represents the 24-h average of these temperature data and red line indicates the accumulation of degree
765 heating weeks (DHWs; $^{\circ}\text{C}$ -weeks) in these data. D) Light intensity ($\mu\text{mol quanta m}^{-2} \text{s}^{-1}$) averaged
766 across two light loggers. Green circle represents location of ADV flow meter during Eulerian
767 estimates. All data were recorded at 15-min intervals from Jan 22 to Feb 13 2020. Aerial photograph
768 is provided by © Google Earth.



769

770 **Figure 2:** Cross-section of coral, algal, and invertebrate diversity observed within the study area. A)
 771 *Dipsastraea* sp.; B) *Stylophora pistillata*; C) *Montipora digitata*; D) *Sarcophyton* sp.; E) *Acropora* sp.;
 772 F) *Pocillopora* sp. G) *Platygyra* sp.; H) *Acropora secale*; I) *Porites attenuata*. J) *Halimeda* sp.; K)
 773 *Holothuria atra*; L) *Dardanus megistos*; M) *Trapezia serenei*; N) Assemblage of *Caulerpa* sp. and
 774 *Laurencia* sp. algae covered in scum sp.; O) *Linckia laevigata*; P) *Stichopus herrmanni*; Q) *Melo*
 775 *amphora*; R) *Tridacna maxima*.

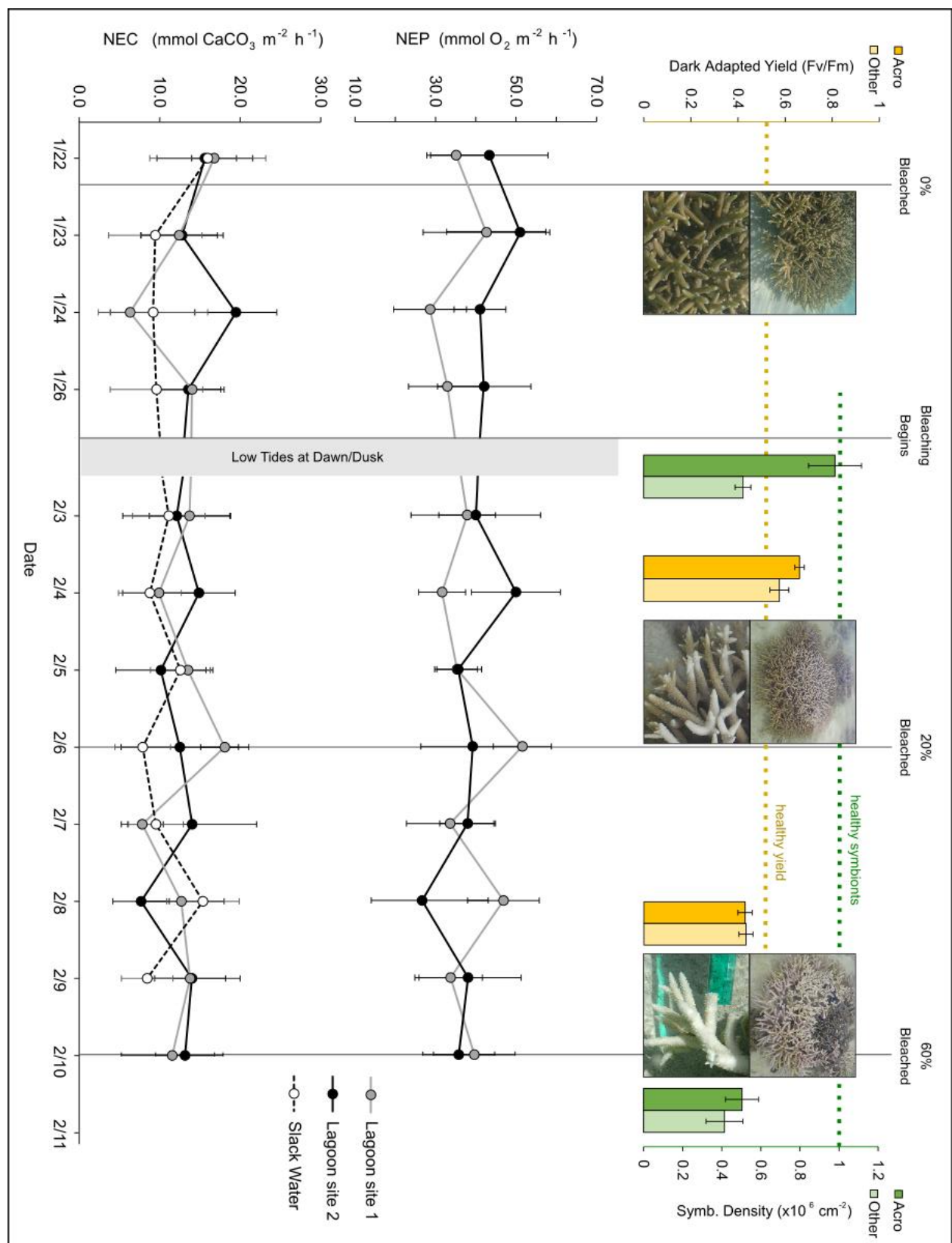


Figure 3: Dark adapted yield (yellow; top left), Symbiodiniaceae densities (green; top right), Rates of net ecosystem production (NEP; middle) and net ecosystem calcification (NEC; bottom) in at Lagoon site 1 (grey), Lagoon site 2 (black), and the larger reef area (Dashed;

780 slack water). Dashed yellow and green lines indicate expected healthy values for dark adapted
781 yield and Symbiodiniaceae densities, respectively. Grey vertical lines indicate the date of
782 photo-quadrat surveys and the resulting percent area of coral that was bleached. NEP and NEC
783 estimates were paused between Jan 26 to Feb 3 due to low tides occurring at dawn and dusk in
784 low light conditions, preventing estimates of NEC. Slack-water estimates are excluded from
785 the NEP data given the large error associated with air-sea gas exchange corrections.

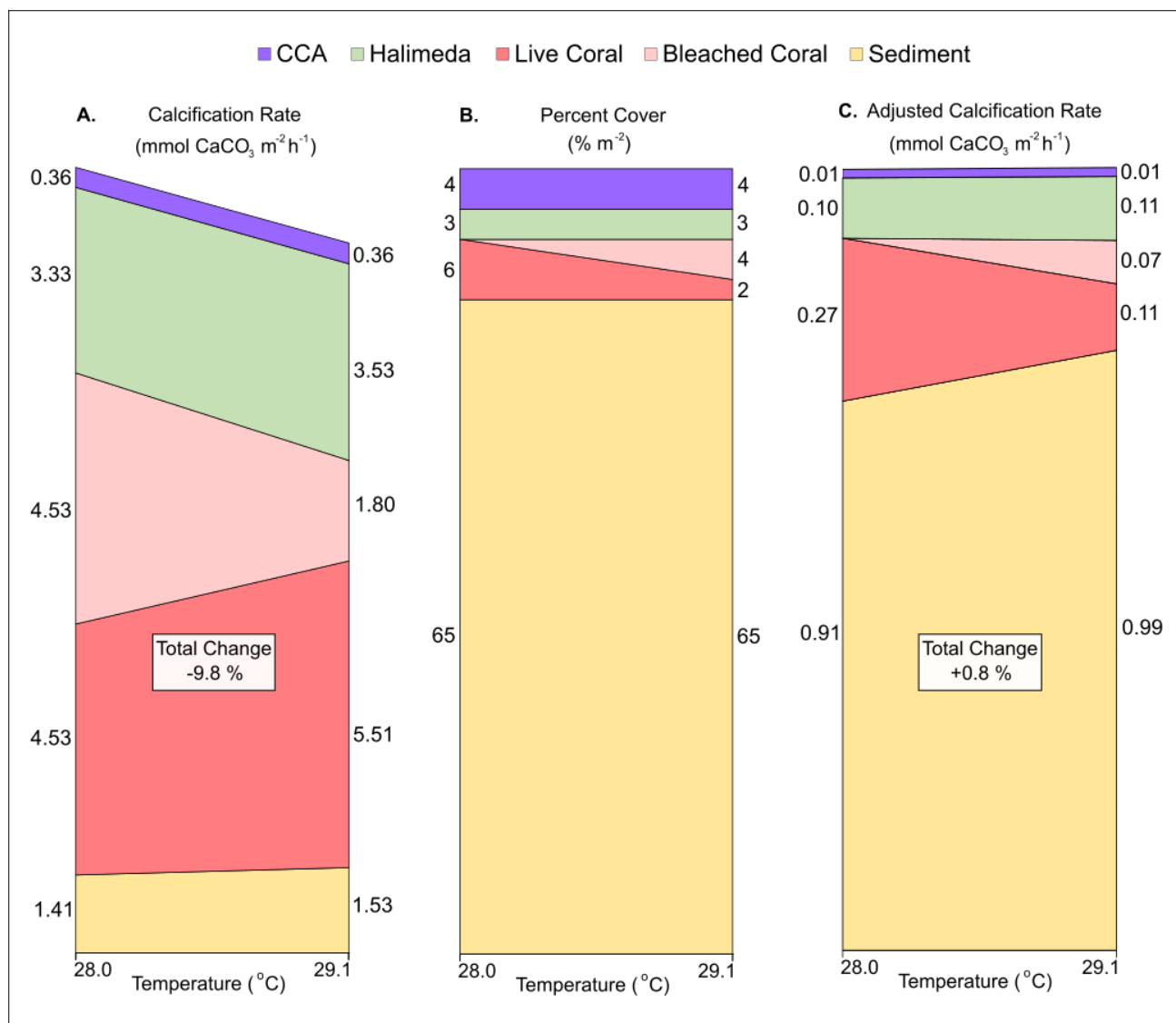


Figure 4: Visualisation of the changes caused by a transition from pre-bleaching (28.0 °C) to bleaching (29.1 °C) temperatures in A) estimated individual organism calcification rates from the literature (converted to mmol CaCO₃ m⁻² h⁻¹), B) percent cover across Lagoon site 1 and Lagoon site 2 combined, and C) the “adjusted the calcification rate” (mmol CaCO₃ m⁻² h⁻¹) calculated by multiplying A. x B. at each temperature. Total change (%) represents the percent difference in the sum of all rates at 29.1 °C relative to 28 °C. Rubble and Other Calcifier categories were assumed to be CCA and *Halimeda* spp., respectively.